Supporting Information

Girouard et al. 10.1073/pnas.0914722107

SI Methods

Ca^{2+} Uncaging and Neuronal Stimulation in Brain Slices. Astrocytic endfoot calcium (Ca^{2+}) in cortical brain slices was elevated by electrical field stimulation (EFS; to stimulate neurons) or by directly uncaging Ca^{2+} in an astrocytic endfoot. Astrocytic endfeet in the same plane of view as the arteriolar lumen were identified. The structure and localization of an endfoot, visualized by imaging Ca^{2+}, were consistent with those observed in individual astrocytes selectively loaded with the fluorescent dye, Lucifer yellow (1), and in cells expressing GFP under the control of the astrocyte-specific glial fibrillary-acid protein promoter. Neurons were stimulated by applying a 50-Hz alternating square pulse of 0.3-ms duration for 3 s (60–150 V) through a pair of platinum wires placed parallel to the brain slice and in the vicinity of the vessel wall. For Ca^{2+} uncaging, a 2.5 × 2.5–μm region of interest (ROI) within an endfoot (zoomed for the duration of one frame) was scanned at a laser intensity about 10× higher than that used for imaging. Reproducible increases in $[Ca^{2+}]_i$ were detected over multiple uncaging events, and no increases in $[Ca^{2+}]_i$ were detected in nonloaded slices. The laser power used for Ca^{2+} imaging was below the threshold for Ca^{2+} uncaging. In both EFS and uncaging paradigms, pharmacological treatment effects were evaluated in paired experiments in which $[Ca^{2+}]_i$ and diameter were determined in the same slice before and after incubating in artificial cerebrospinal fluid (aCSF) containing drug or elevated K^+ (isomolar substitution for Na^+) for 10 min. Matched time controls were also performed.

Endfoot Ca^{2+} Quantification. Estimates of $[Ca^{2+}]_i$ were made using the F_{max} equation (2) (Eq. S1)

$$Ca^{2+} = K_d \frac{F/F_{max} - 1/Rf}{1 - F/F_{max}} \qquad [S1]$$

where F is fluorescence measured within a ROI (15 × 15 pixels or 1.8 × 1.8 μm) positioned on an endfoot, F_{max} is the fluorescence intensity of Fluo-4 at a saturating free Ca^{2+} concentration, K_d is the dissociation constant of Fluo-4 (340 nM) (3), and Rf (= 100) is this indicator's ratio of maximum to minimum fluorescence measured in vitro at saturating and zero Ca^{2+} concentrations (4). F_{max} was obtained individually for each slice by adding the Ca^{2+} ionophore, ionomycin (10 μM), and 20 mm external Ca^{2+} to the aCSF at the end of the experiment. Fractional fluorescence (F/F_0) was determined by dividing the fluorescence intensity (F) within a ROI by a mean fluorescence value (F_0) determined from 15 images collected before stimulation.

Diameter Measurements of Isolated Pressurized Parenchymal Arterioles. Brains from 3- to 5-month-old male C57BL6 mice were removed and placed into cold Mops-buffered saline [145 mM NaCl, 3 mM KCl, 1.2 mM NaH_2PO_4, 1.17 mM $MgSO_4$, 2 mM $CaCl_2$, 5 mM glucose, 3 mM Mops (pH 7.4), 10 mg/mL BSA]. For pressurized arteriole experiments, parenchymal arterioles (25–30 μm external diameter) were dissected from the middle cerebral artery (MCA) at a minimum of 500 μm distal to their point of origin and cannulated to resistance-matched micropipettes on an arteriograph system. Parenchymal arterioles were pressurized (40 mmHg) using an electronic servo-pressure transducer (Living Systems Instruments) and continuously perfused with oxygenated, prewarmed (37 °C) aCSF. Vessel diameter was continuously monitored using a CCD camera and edge-detection software (IonOptix). Arteriole viability was tested at the conclusion of the experiment by depolarizing with 60 mM K^+ to induce constriction and then, bathing in a Ca^{2+}-free solution containing 100 μM papaverine (a phosphodiesterase inhibitor) to induce maximal dilation.

In Vivo Experiments. Male C57BL6 mice (2–3 months old) were used routinely and as a control for α1-KO mice. Male Friend leukemia virus B (FVB) mice were used as a control for *Slo*$^{-/-}$ mice. Mice were anesthetized with isoflurane (maintenance, 2%) in oxygen and artificially ventilated through a tracheotomy (SAR-830; CWE) (5, 6). A catheter was inserted into the femoral artery for recording mean arterial pressure and collecting blood samples. Body temperature, recorded rectally was maintained at 37 °C with a feedback-controlled heating blanket. A 2 × 2-mm craniotomy was performed to expose the somatosensory cortex, the dura was removed, and the site was superfused with aCSF (37 °C). After surgery, anesthesia was maintained with urethane (750 mg/kg ip) and chloralose (50 mg/kg ip), and the depth of anesthesia was verified by testing corneal reflexes and motor responses to tail pinch (5–7). Cortical cerebral-blood flow (CBF) was monitored in the cranial window by laser-Doppler flowmetry (8) using a laser-Doppler probe (Perimed) connected to a computerized data-acquisition system (PowerLab). The probe (0.6-mm diameter tip), which measures flow (expressed in arbitrary units) in a cortical volume of 0.5–1.0 mm (9), was mounted on a micromanipulator and positioned ~0.5 mm above the pial surface at a site distant from visible pial arteries. CBF was expressed as percent increase relative to the resting level. Zero values were obtained after the heart was stopped with an overdose of isoflurane. Because laser-Doppler flowmetry measures fractional increases in CBF in a cortical volume (<1 mm^3), it does not measure changes in individual arterioles but instead reflects the aggregate increase. Accordingly, increases in blood flow measured by laser-Doppler flowmetry cannot be quantitatively mapped to dilations of individual arterioles. However, the qualitative effects of pharmacological agents should be comparable, allowing similar conclusions to be drawn.

A functional hyperemic response was induced in the region of the left somatosensory cortex exposed in the cranial window by stroking the right vibrissae (cut to a length of 10 mm) at a frequency of about 3 Hz for 1 min (6, 8). The cranial window was first superfused with aCSF solution for 30 min, and then, CBF responses were recorded. The response to whisker stimulation was tested three times at 10-min intervals before and 20 min after superfusion of the cortex with pharmacological agents, as detailed in the text. All pharmacological agents were dissolved in aCSF solution, except paxilline, which was first dissolved in DMSO (final DMSO concentration = 0.01%).

Reagents. The thromboxane agonist, U46619, was obtained from Calbiochem. Paxilline (Sigma), an indole diterpene, is a commonly used, selective Ca^{2+}-sensitive potassium (BK)-channel blocker (10). The low molecular weight (435.6) paxilline was chosen over iberiotoxin, a scorpion-venom peptide, because it is more likely to effectively penetrate the slice and cortex and its affinity is not significantly affected by the nature of the β-subunit of the BK channel (10). Paxilline has been shown to maximally block BK currents in isolated smooth-muscle cells at 300–500 nM (IC_{50} 97 nM), depending on the preparation and cell type used (11, 12). To produce significant block of BK channels and to minimize potential high concentration off-target effects, we used paxilline at 1 μM in brains slices and in vivo. Paxilline at this

concentration has no effects on CBF (Fig. 5) or neurological function (10) in the absence of the BK channel. External barium ions have been shown to block strong inward rectifier potassium channels in cerebral artery smooth-muscle cells with a half-block constant of about 10 μM at −40 mV (13) and prevent potassium-induced dilations (14, 15). At 100 μM, external barium has little or no effect on voltage-dependent calcium channels, voltage-dependent potassium channels, or BK channels (16). Fluo-4 AM and pluronic acid were obtained from Invitrogen. 1-[4,5-dimethoxy-2-nitrophenyl]-EDTA-AM (DMNP-EDTA-AM) ester was obtained from Interchim. All other chemicals were obtained from Sigma-Aldrich.

Statistics. All data are expressed as mean ± SEM. Differences among groups were analyzed using ANOVA and Tukey's test for multiple comparisons, and differences between two means were analyzed using the appropriate Student's t test. P values < 0.05 were considered statistically significant. $[Ca^{2+}]_i$ data and arteriole diameter in brain slices were analyzed using custom-designed software created by A. Bonev (Burlington, VT).

1. Zonta M, et al. (2003) Neuron-to-astrocyte signaling is central to the dynamic control of brain microcirculation. *Nat Neurosci* 6:43–50.
2. Maravall M, Mainen ZF, Sabatini BL, Svoboda K (2000) Estimating intracellular calcium concentrations and buffering without wavelength ratioing. *Biophys J* 78: 2655–2667.
3. Yasuda R, et al. (2004) Imaging calcium concentration dynamics in small neuronal compartments. *Sci STKE* 219:pl5.
4. Woodruff ML, et al. (2002) Measurement of cytoplasmic calcium concentration in the rods of wild-type and transducin knock-out mice. *J Physiol* 542:843–854.
5. Girouard H, Park L, Anrather J, Zhou P, Iadecola C (2006) Angiotensin II attenuates endothelium-dependent responses in the cerebral microcirculation through nox-2-derived radicals. *Arterioscler Thromb Vasc Biol* 26:826–832.
6. Girouard H, Park L, Anrather J, Zhou P, Iadecola C (2007) Cerebrovascular nitrosative stress mediates neurovascular and endothelial dysfunction induced by angiotensin II. *Arterioscler Thromb Vasc Biol* 27:303–309.
7. Girouard H, Lessard A, Capone C, Milner TA, Iadecola C (2008) The neurovascular dysfunction induced by angiotensin II in the mouse neocortex is sexually dimorphic. *Am J Physiol Heart Circ Physiol* 294:H156–H163.
8. Haberl RL, Heizer ML, Ellis EF (1989) Laser-Doppler assessment of brain microcirculation: Effect of local alterations. *Am J Physiol* 256:H1255–H1260.
9. Niwa K, Haensel C, Ross ME, Iadecola C (2001) Cyclooxygenase-1 participates in selected vasodilator responses of the cerebral circulation. *Circ Res* 88:600–608.
10. Imlach WL, et al. (2008) The molecular mechanism of "ryegrass staggers," a neurological disorder of K+ channels. *J Pharmacol Exp Ther* 327:657–664.
11. Tammaro P, Smith AL, Hutchings SR, Smirnov SV (2004) Pharmacological evidence for a key role of voltage-gated K+ channels in the function of rat aortic smooth muscle cells. *Br J Pharmacol* 143:303–317.
12. Li G, Cheung DW (1999) Effects of paxilline on K+ channels in rat mesenteric arterial cells. *Eur J Pharmacol* 372:103–107.
13. Quayle JM, McCarron JG, Brayden JE, Nelson MT (1993) Inward rectifier K+ currents in smooth muscle cells from rat resistance-sized cerebral arteries. *Am J Physiol* 265: C1363–C1370.
14. Knot HJ, Zimmermann PA, Nelson MT (1996) Extracellular K(+)-induced hyperpolarizations and dilatations of rat coronary and cerebral arteries involve inward rectifier K(+) channels. *J Physiol* 492:419–430.
15. Zaritsky JJ, Eckman DM, Wellman GC, Nelson MT, Schwarz TL (2000) Targeted disruption of Kir2.1 and Kir2.2 genes reveals the essential role of the inwardly rectifying K(+) current in K(+)-mediated vasodilation. *Circ Res* 87:160–166.
16. Nelson MT, Quayle JM (1995) Physiological roles and properties of potassium channels in arterial smooth muscle. *Am J Physiol* 268:C799–C822.

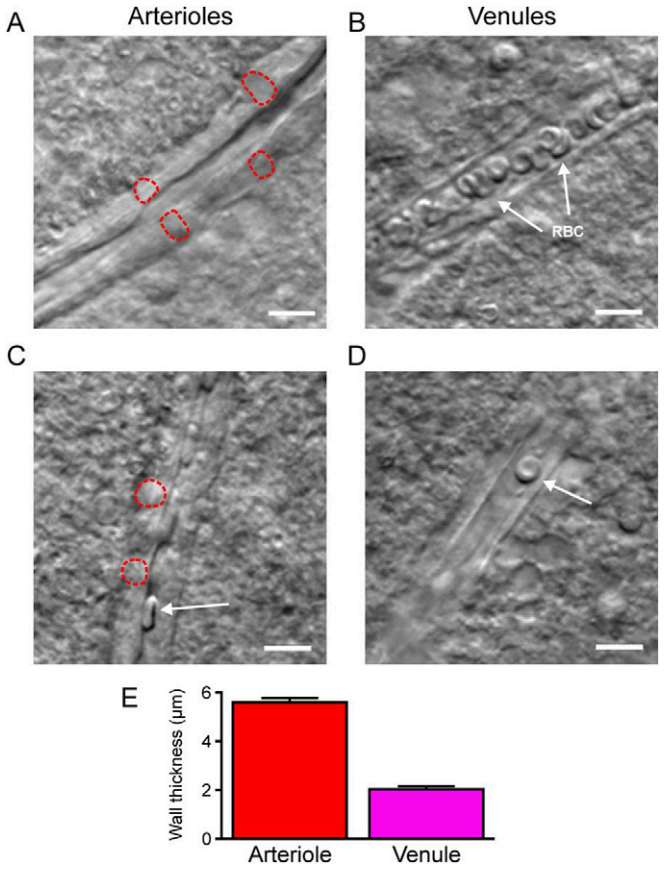

Fig. S1. Arterioles (*Left*; *A* and *C*) and venules (*Right*; *B* and *D*) in mouse brain slices. The thickness of the vessel walls reflects the presence (arteriole) or absence (venule) of a smooth-muscle cell layer. Individual smooth-muscle cells could be easily identified in the arterioles; for illustration, several myocytes are circled with dashed lines. RBCs are trapped in the arterioles and venules (white arrows). The mean wall thickness for arterioles and venules is shown in *E*. (Scale bar: 10 μm.)

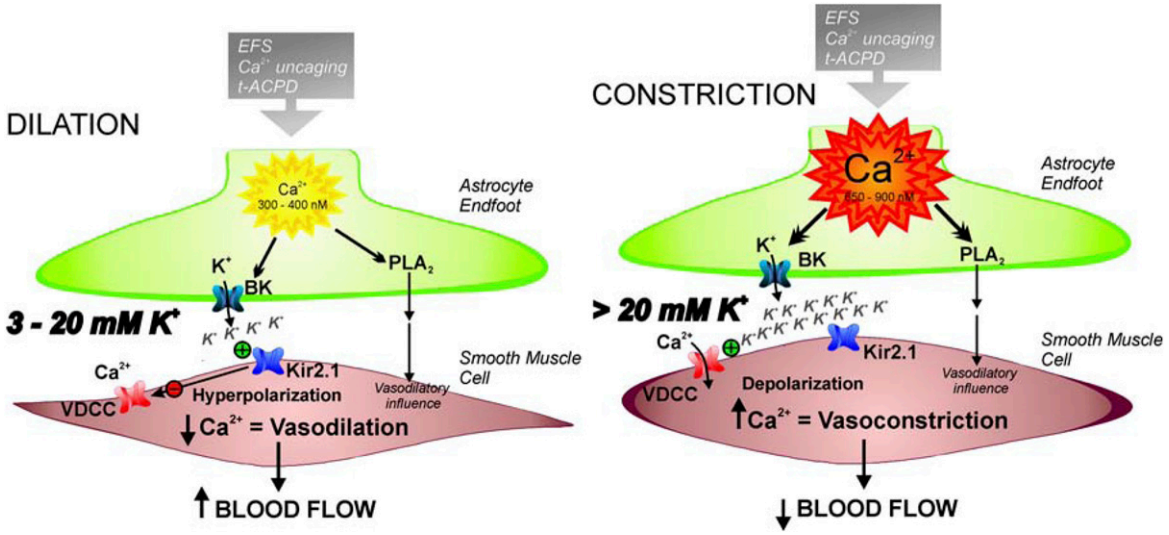

Fig. S2. Astrocytic endfoot Ca^{2+} activates large-conductance BK channels, which determine the vascular response to neuronal activity. (*Left*) Moderate elevation of endfoot $[Ca^{2+}]_i$ (300–400 nM) activates BK channels, releasing K^+ ions into the perivascular space to increase local $[K^+]_o$ to <20 mM. $[K^+]_o$ activates K_{ir} channels in the arteriolar smooth muscle cell (SMC) membrane to hyperpolarize the SM membrane potential (1), closing voltage-dependent Ca^{2+} channels (VDCCs) and causing vasodilation. (*Right*) Larger increases in endfoot $[Ca^{2+}]_i$ (>700 nM) switch the polarity of the vascular response from dilation to constriction by releasing more K^+ ions into the perivascular space, causing SM depolarization and vasoconstriction. Blocking BK channels reduces the evoked dilation and switches the evoked constriction to a modest dilation. Blocking K_{ir} channels eliminates the BK-channel–dependent dilation but does not affect the constriction. Also shown is the Ca^{2+}-dependent activation of cytoplasmic phospholipase A2 (PLA_2), which presumably provides a parallel pathway for dilation but not constriction.

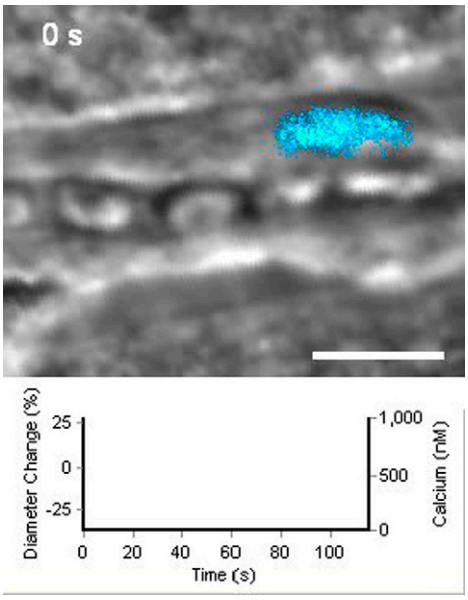

Movie S1. Arteriolar dilation induced by uncaging normal levels of Ca^{2+} in an astrocytic endfoot abutting an arteriole in the slice shown in Fig. 1 *A* and *B*, *Left*. The time course of changes in Ca^{2+} and diameter are depicted graphically below (14× normal speed).

Movie S1

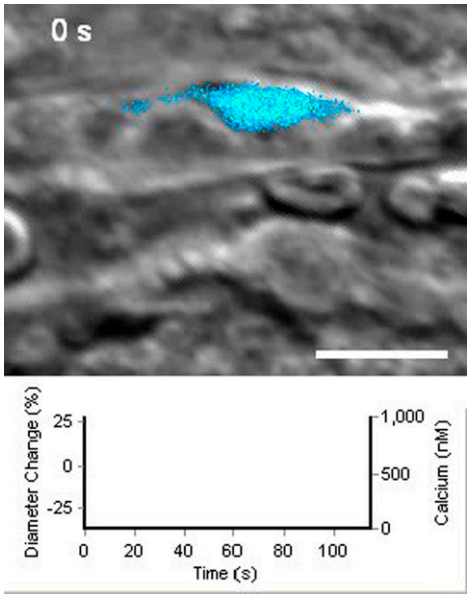

Movie S2. Arteriolar constriction induced by uncaging high levels of Ca^{2+} in an astrocytic endfoot abutting an arteriole in the slice shown in Fig. 1 *A* and *B*, *Right*. The time course of changes in Ca^{2+} and diameter are depicted graphically below (14× normal speed).

Movie S2